Computational Study on the Hemodynamics of the Bypass Shunt Directly Connecting the left Ventricle to a Coronary Artery

Eun Bo Shim*
Department of Mechanical Engineering, Kangwon National University,
Hyoja-Dong, Chucheon, Kangwon-Do 200-701, Republic of Korea

Byung Jun Lee
The Research Institute of Mechanical Technology, Pusan National University,
Jangjeon-Dong, Geumjeong-Gu, Busan 609-735, Republic of Korea

Hyung Jong Ko
Department of Mechanical Engineering, Kumoh National Institute of Technology,
Shinpyung-Dong, Kumi, Kyungbuk 730-701, Republic of Korea

A shunt from the left ventricle to the left anterior descending artery is being developed for coronary artery occlusive disease, in which the shunt or conduit connects the the left ventricle (LV) with the diseased artery directly at a point distal to the obstruction. To aid in assessing and optimizing its benefit, a computational model of the cardiovascular system was developed and used to explore various design conditions. Computational fluid dynamic analysis for the shunt hemodynamics was also done using a commercial finite element package. Simulation results indicate that in complete left anterior descending artery (LAD) occlusion, flow can be returned to approximately 65% of normal, if the conduit resistance is equal for forward and reverse flow. The net coronary flow can increase to 80% when the backflow resistance is infinite. The increases in flow rate produced by asymmetric flow resistance are enhanced considerably for a partial LAD obstruction, since the primary effect of resistance asymmetry is to prevent leakage back into the ventricle during diastole. Increased arterial compliance has little effect on net flow with a symmetric shunt, but considerably augments it when the resistance is asymmetric. The computational results suggest that an LV-LAD conduit will be beneficial when the resistance due to artery stenosis exceeds 27 PRU, if the resistance is symmetric. Fluid dynamic simulations for the shunt flow show that a recirculating region generated near the junction of the coronary artery with the bypass shunt. The secondary flow is induced at the cutting plane perpendicular to the axis direction and it is in the attenuated of coronary artery.

Key Words : Computational Model, Coronary Circulation, LV-LAD Bypass Shunt, Lumped Parameter Model, Device Efficiency

1. Introduction

Current methods for treating coronary artery

* Corresponding Author,
E-mail : ebshim@kangwon.ac.kr
TEL . +82-33-250-6318; **FAX :** +82-33-250-6013
Department of Mechanical Engineering, Kangwon National University, Hyoja-Dong, Chucheon, Kangwon-Do 200-701, Republic of Korea. (Manuscript **Received** August 24, 2004; **Revised** March 11, 2005)

disease, using either coronary artery bypass graft (CABG) or coronary angioplasty, are generally successful and continue to be improved. Despite the excellent success of these methods, a significant number of patients experience repeated occlusion and ultimately reach a state in which they have few remaining alternatives. The persistence of this patient subgroup despite the most recent advances in existing methods has motivated the search for entirely new treatment modalities, in-

cluding TMR (transmyocardial revascularization) (Frazier et al., 1999).

Recently, direct shunt implantation from the left ventricle (LV) to the LAD (LV-LAD) has been proposed as an alternative, and is now being investigated widely using experimental approaches (Tweden et al., 2000 ; Suehiro et al., 2001 ; Boekstegers et al., 2002 ; de Zeeuw et al., 2004). As shown in Fig. 1, this method bypasses the region of obstruction using a direct shunt between the left ventricle (LV) and the region distal to the obstructed vessel, considered the LAD artery here. The success of this approach is based on the hypothesis that the forward flow generated during cardiac systole exceeds the reverse flow, from the coronary arteries into the left ventricle, during diastole. Tweden et al.(2000) proposed a basic mechanism for this device in an animal experiment. Boekstegers et al.(2002) delineated a valve-like mechanism during diastole for this procedure. Suehiro et al.(2001) investigated the global cardiac function when this device was implanted in dogs. de Zeeuw et al.(2004) also examined experimentally whether the augmented coronary compliance would improve the net forward shunt flow in a cardiac cycle. Although much useful experimental data concerning this method has been obtained, the conditions for optimal coronary artery perfusion remain unclear.

Many computational studies that explain the coronary hemodynamics for the normal coronary circulation have been conducted. Computational approaches can be an effective means to delineate the coronary circulation in normal or pathological states. Beyar et al.(1989, 1993) provided computational results for the transmyocardial coronary flow patterns during normal and ischemic conditions, which are complex and relatively inaccessible to measurements. Schreiner et al. (1990) used a mathematical model to represent the vascular bed of the left coronary circulation as arterial, capillary, and venous compartments. Rooz et al.(1985) delineated the epicardial coronary blood flow, including the presence of stenoses and aortocoronary bypasses.

Due to the complexity of animal testing, and the natural variability experienced in biological experiments, there is a need to develop rapid, systematic analysis and optimization methods. Here, we develop a computational model to explore different design conditions in the case of a LV-LAD conduit. Our goal was to identify promising approaches that might then be evaluated further in experiments on test animals. We consider the dimensions of the connecting conduit, the benefits of producing asymmetric flow resistance through it, and the effects of variation in the arterial compliance. The computational simulation of blood flow through the bypass shunt is also presented in this study. A commercial finite element package is used to study the detailed flow patterns within the shunt and adjacent artery and to identify regions of flow separation.

2. Methods

The proposed procedure introduces a direct connection between the left ventricle and a distal segment of the obstructed artery by inserting a direct shunt between the left ventricle and the coronary artery through the myocardium (Fig. 1). For optimal design of the shunt, it is necessary to investigate the effect of local parameters, such as the shunt angle θ and shunt diameters D_1 and D_2. The shunt or conduit may be a simple tube of uniform internal diameter, or shaped so that it creates conditions favoring flow into the coronary arterial segment rather than in the reverse direction, as shown in the figure (in this case, the shunt diameter on the coronary artery side, D_2, is wider
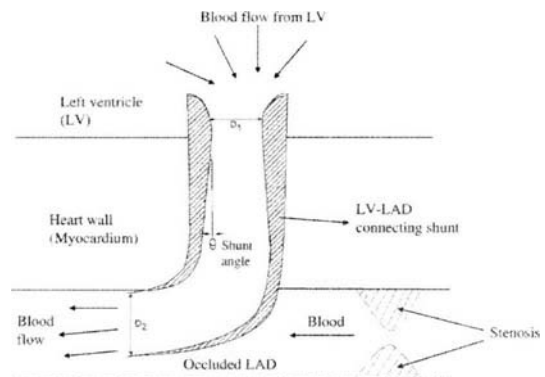

Fig. 1 Schematic of the proposed surgical procedure

than on the ventricle side, D_1).

To investigate the hemodynamic effects of conduit insertion, we implemented a computational code capable of simulating the dynamics of the coronary circulation. We compared the model predictions with available experimental data to validate the simulation.

In general, the hemodynamics of vessels can be represented by the relationship between blood pressure and blood flow rate in the cardiovascular system. In a lumped model, the hemodynamic elements of the coronary system are expressed as a series of equivalent elements in an electric circuit, as shown in Fig. 2. Each compartment is characterized by an inflow resistance, R_i, expressed in peripheral resistance units (1 PRU = 1 mmHg·s/ml), an external pressure (or biased pressure) to vessel wall in mmHg, the compliance or, in the electrical analogy, a capacitance, C, in ml/mmHg, and an outflow resistance, R_o. In our model, the basic coronary circulation consists of three compartments: the coronary arteries, coronary capillaries, and coronary veins, as shown in Fig. 3. The input data for the coronary system are the aortic, right atrium, and left ventricle pressures that were given in our previous model of the entire cardiovascular (CV) system (Heldt, et al., 2002; Shim et al., 2002). In order to simulate the effects of an LV-LAD shunt, the left ventricle is connected to the LAD via a pair of resistor-diode pairs, one to convey flow from the LV to the LAD ("forward" flow) and another to convey flow from the LAD to the LV ("reverse" flow). Diodes are introduced to ensure unidirectional flow through each pathway. Different resistance values can be assigned to each path to examine the potential benefit of directional asymmetry in flow resistance (Fig. 3). The application of Kirchhoff's law to each node in the lumped parameter hemodynamic model leads to the following differential equation for mass conservation.
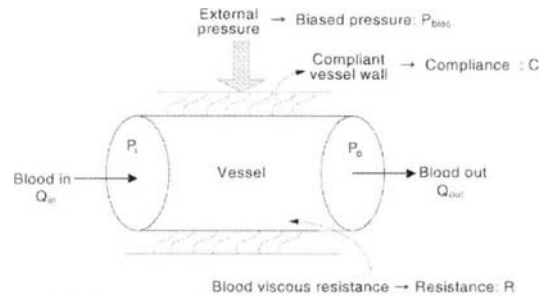
(a) Hemodynamic elements of a blood vessel
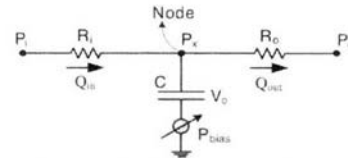
(b) Equivalent electric circuit

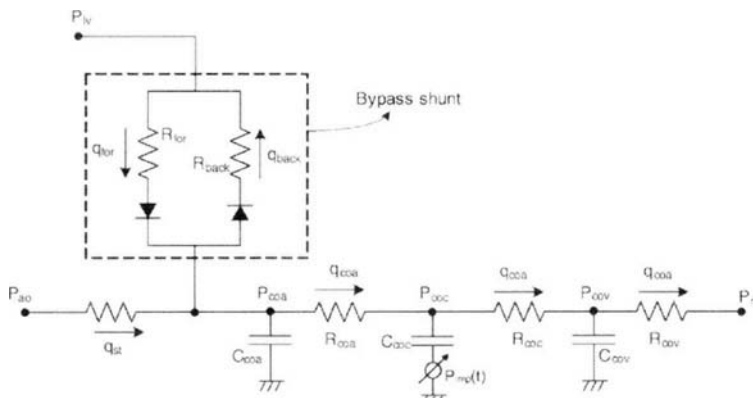**Fig. 2** Electrical analog of vascular hemodynamic elements

Fig. 3 Schematic of a lumped parameter model of the coronary circulation with a bypass shunt connecting the left ventricle to the coronary artery (ao : aorta, coa : coronary arteries, coc : coronary capillaries, cov : coronary veins, ra : right atrium, lv : left ventricle, st : stenosis, imp : intra-myocardium)

$$\frac{dV}{dt}=Q_{in}-Q_{out} \qquad (1)$$

where

$$Q=(P_i-P_o)/R \qquad (2)$$

$$(P-P_{bias})=V/C \qquad (3)$$

In these equations, V is the volume of a compartment, Q is the flow rate, P is the pressure, P_{bias} is the external squeezing on the vessel wall, and C is the capacitance. A new volume can be calculated from the flow rates derived using Equation (2). After obtaining the volume, the pressures at the nodes are calculated using Equation (3). Application of this formula to the other nodes leads to a matrix equation of the form :

$$d\mathbf{p}/dt=\mathbf{Ap}+\mathbf{b} \qquad (4)$$

Here, $\mathbf{p}$ is the vector containing all the compartmental pressures, $\mathbf{A}$ represents the time constants for the exchange between compartments, and $\mathbf{b}$ is the input to the system. This initial value problem of ordinary differential equations is solved using a fourth order Runge-Kutta method, yielding the pressures within each compartment and the flows between compartments, both as functions of time. A more detailed presentation of the model and the associated equations can be found in Appendix A for the coronary vessel network. The values for each of the model parameters, and how they are selected, are discussed later and in Table 1.

The reference value of conduit resistance is obtained by assuming Poiseuille flow (fully developed, steady, and laminar). This should be viewed as a rough estimate of the actual flow resistance through the reference conduit, since the effects of unsteadiness, flow separation, and small variations in internal geometry (among other factors) could exert a significant influence on this value. The flow rate, Q, through the conduit (or shunt) under this assumption is expressed as follows :

$$Q=\frac{A^2\Delta P}{8\,\pi\mu L} \qquad (5)$$

Here, A, ΔP, μ, and L represent the cross-sectional area, pressure drop, fluid viscosity, and conduit length, respectively. From this relation, we can estimate the conduit resistance :

$$R_{sh}=\frac{\Delta P}{Q}=\frac{8\,\pi\mu L}{A^2} \qquad (6)$$

Using typical values for the conduit diameter ($D=2$ mm), length ($L=2$ cm), and blood viscosity ($\mu=0.003$ kg/(m·s)), the calculated resistance is 1.146 PRU (Tweden et al., 2000). In this study, we want to simulate the flow in the distal LAD. Any LV-LAD shunt will generally be placed about 2/3 of the way down the vessel. The estimated flow rate was approximately 0.667 ml/sec (Tweden et al., 2000) due to the existence of the small arteries in the proximal LAD. Since normal values for the LAD flow rate are in the range of 1 ml/s, we adjusted the coronary arteriolar resistance, R_{coa}, and coronary capillary resistance, R_{coc}, until the baseline flow rate was 2/3 of the total LAD flow rate, or approximately 0.667 ml/sec in the absence of any constriction (Schreiner et al., 1990). The ratio of arteriolar to capillary resistance was taken to be 10 and assumed to be constant. Since our interest is in

Table 1 Parameter estimation for the computational model of the coronary circulation

Compartment	R_{in} (PRU)	R_{out} (PRU)	C (ml/mmHg)	V_0 (ml)	Sources
Coronary arteries	Variable	13.5 (R_{coa})	0.003	0.0	Schreiner et al., 1990
Coronary capillaries	13.5 (R_{coa})	1.37 (R_{coc})	0.4	25	Schreiner et al., 1990
Coronary veins	1.37 (R_{coc})	0.6 (R_{cov})	0.25	3.4	Schreiner et al., 1990
Resistance due to stenosis	Variable				
Bypass shunt resistance	Variable				
Intra-myocardium Pressure	$P_{imp}(t)=0.75\times P_{lv}(t)$				Schreiner et al., 1990 & Beyar, 1993
Reference coronary venous volume	$V_{cov}^0=25$ ml				Schreiner et al., 1990
Reference coronary compliance	$C_{cov}^0=0.25$ ml/mmHg				Schreiner et al., 1990

simulating advanced disease, we assumed that the peripheral bed was dilated maximally, which we estimated to correspond to the case in which the resistance was reduced to 20% of normal. Consequently, the flow rate through the unobstructed vessel was 3.33 ml/s, which is five times as large as the assumed normal flow rate when there is no proximal obstruction. The values of the arteriolar and capillary resistance that produced this flow rate were $R_{coa}=13.5$ PRU and $R_{coc}=1.35$ PRU, respectively.

3. Results and Discussion

Since blood flow through the coronary circulation is small relative to the total circulation, the coronary circulation has little influence on the overall distribution of blood flow (Feigl, 1989). Therefore, we assume that the aortic and left ventricular pressures obtained using our previous computational code of the cardiovascular system are the main determinants of coronary blood flow.

The aortic and left ventricle pressures obtained from our previous model of the cardiovascular system (Shim et al., 2002) are represented in Fig. 4. During systole, the coronary capillary flow rate decreases due to the increased resistance res-

ulting from myocardial contraction, whereas flow through the coronary veins increases due to compression of the capillaries (Fig. 5(a)). For the purpose of verification, we simulated the coronary circulation in a normal state and compared our results with the published results of Schreiner et al. (1990). The capillary and venous volumes
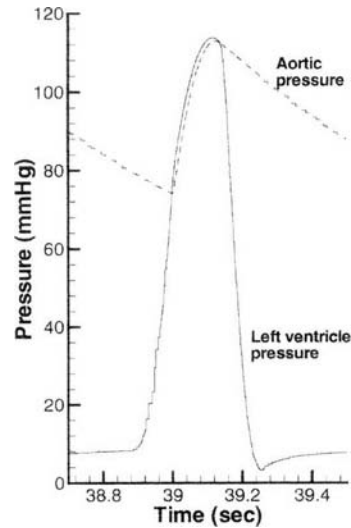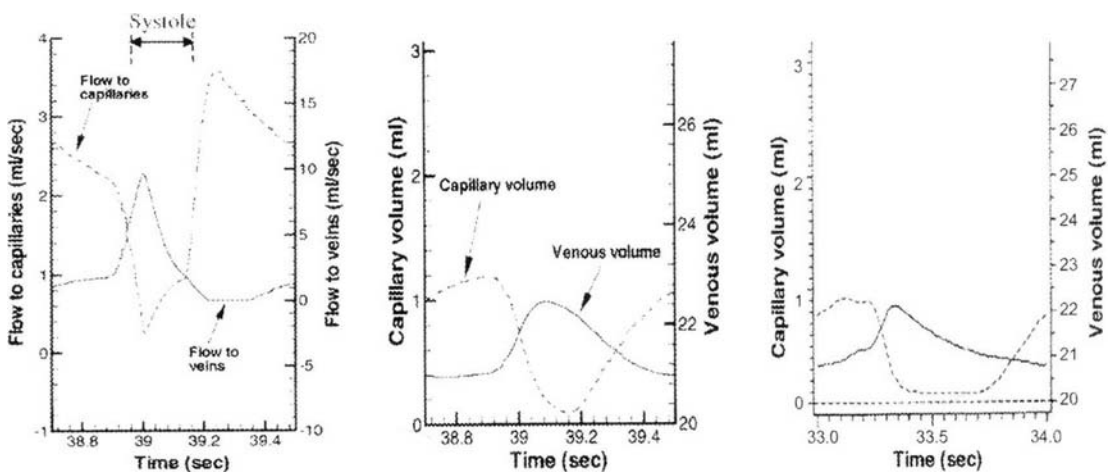
Fig. 4 Temporal variation in the left ventricular and aortic pressures obtained from our previous cardiovascular system model (Shim et al., 2002)

(a) Flow rate to capillaries and veins in the present calculation

(b) Coronary capillary and venous volume the present in calculation

(c) Coronary capillary and venous volume in a previous computation (Schreiner et al., 1990)

Fig. 5 Flow rate and volume changes during a cardiac cycle for normal coronary circulation

Table 2 The minimum and maximum values of the capillary and venous blood volumes

		This study	Schreiner et al. (1989)
Capillary blood volume	Minimum value	0.09 ml	0.08 ml
	Maximum value	1.18 ml	0.94 ml
Venous blood volume	Minimum value	20.97 ml	20.80 ml
	Maximum value	22.46 ml	22.15 ml

vary in a manner similar to the flow rate variation shown in Fig. 5(b). The temporal variation in the patterns of the capillary and venous volumes is comparable to that in Fig. 5(c) in Schreiner et al.(1990). The minimum and maximum blood volumes of the capillary and veins in our study are also similar to those reported in Schreiner et al.(1990), as represented in Table 2.

For a fully occluded LAD, we compared our computational results with experimental measurements in a dog, following placement of a conduit, executed by Suehiro et al.(2001). They performed this experiment for 27–32 kg dogs with a heart rate of 131 ± 10 bpm (beats per minute). In the simulation, we assumed a 30 kg dog with a heart rate of 121 bpm. The computed aortic pressure and coronary arterial flow (q_{coa}) are shown in Fig. 6, with the experimental results. Except for the duration of systole in some parts, all the flow and pressure data were in good agreement with the experimental results.

In our simulations, we varied the resistance of the stenosis, R_{st}, to simulate conditions ranging from total occlusion $(R_{st} = \infty)$ to completely open and healthy $(R_{st} = 0)$. Fig. 7 shows the flow rates in the case with total occlusion. Here, the subscripts 'sh' and 'coa' correspond to the conduit and coronary arterioles, respectively. The numerical results show a large peak in the forward flow during systole and a smaller, but still significant, negative flow during diastole, essentially out-of-phase with the coronary artery flow in an unobstructed system. In case of the normal coronary circulation, blood flow in the coronary artery is lower during systole as compared to diastole (Fig. 5(a)). The reason for this is strong compression of the left ventricular muscle around the intramuscular coronary vessels during cardiac contraction. During diastole, the cardiac muscles
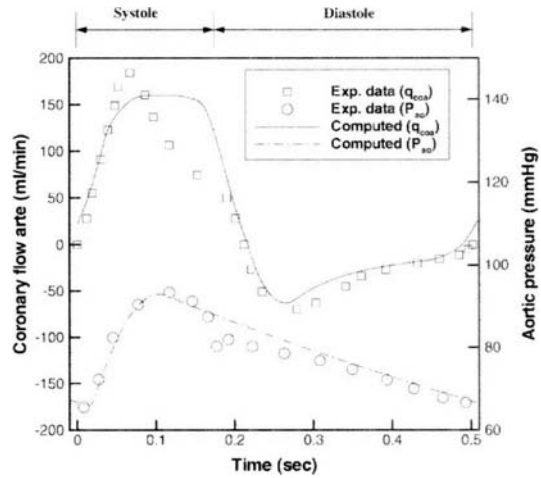

Fig. 6 Computed LAD flow rate (Q_{coa}) and the aortic pressure compared with the dog experiment by Suehiro et al.(2001) during one cardiac cycle
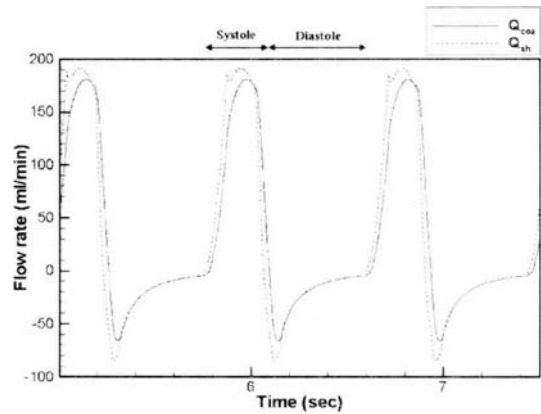

Fig. 7 Computed flow rates of the LAD (Q_{coa}) and shunt (Q_{sh}) with the proximal LAD totally occluded and the conduit in place

relax and no longer impede blood flow through the ventricular capillaries, so that blood flows more freely. Unlike the normal coronary circula-
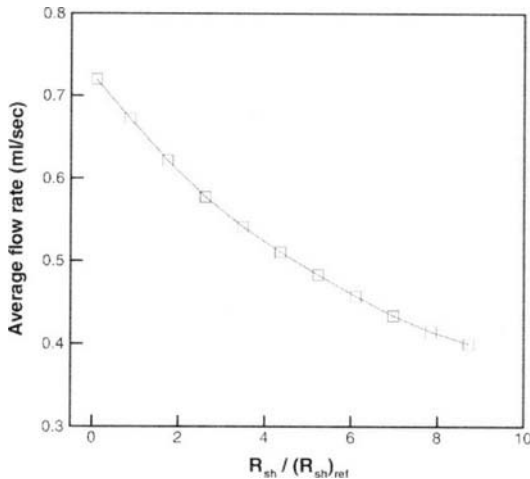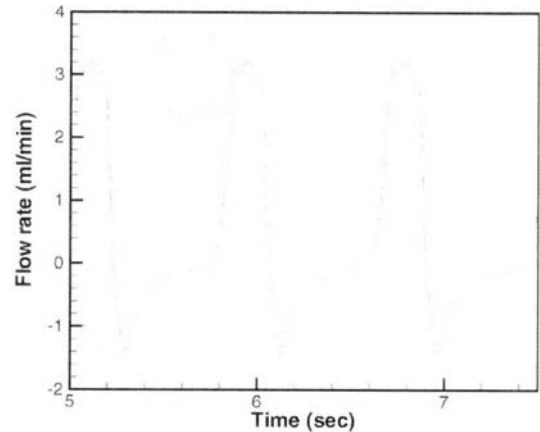
Fig. 8 Variation in the average LAD flow rate as a function of conduit resistance with the coronary artery totally occluded. Here, (R_{sh}) ref is the reference shunt resistance $(= 1.146$ PRU) when the diameter and length of the shunt are 2 mm and 2 cm, respectively

(a) $C_{coa} = 0.003$

(b) $C_{coa} = 0.03$

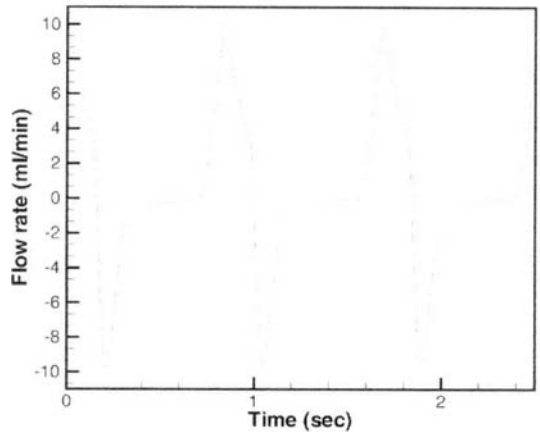**Fig. 9** Temporal variation in the LAD flow for two different arterial compliances

tion, the coronary blood flow is synchronized with the LV pressure (high coronary flow in high LV pressure) in case of the LV-LAD shunt with coronary artery occluded because of the direct connection from the LV to the coronary artery.

An initial series of computations were performed to establish the relation between conduit resistance and flow rate through the conduit (Fig. 8). In this case, the LAD is fully occluded. According to the figure, the increase in conduit resistance induces a decrease in the net flow rate through the conduit, as one would expect. Consequently, this plot indicates that the minimum conduit resistance produces the greatest flow with LAD occlusion. We also found that distal vessels must be dilated maximally for effective myocardial perfusion.

To test the effect of the compliance of the coronary artery, we performed calculations for two values of compliance, as represented in Fig. 9 : a normal value (0.003 ml/mmHg) and a higher value (0.03 ml/mmHg). The peak positive and negative flow rates with the higher epicardial capacitance are larger than those with the lower epicardial capacitance. However, the net (cycle-

averaged) flow rate during one cardiac cycle is nearly identical in these two cases. Blood is simply shunted into and out of the arterial capacitance.

Since any blood that returns to the LV during diastole is essentially lost to the coronary circulation, it would seem advantageous to design a conduit tube that favors forward flow over reverse flow. As shown in Fig. 1, the LV-LAD conduit might be tapered, with a smaller diameter at the side of the LV. This would produce a resistor with low forward (into the coronary artery) resistance and a higher reverse (out-of the coronary artery) resistance.

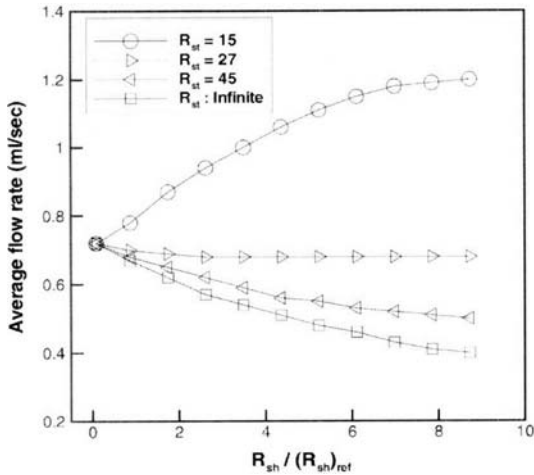Fig. 10 shows that flow rate increases as the

Fig. 10 Average LAD flow rate versus the conduit resistance in several cases of stenotic resistance. Note that a stenosis resistance of 15, 27, and 45 PRU represents a diameter reduction of about 66, 71, and 74%, respectively. Here, R_{sh} is in PRU.
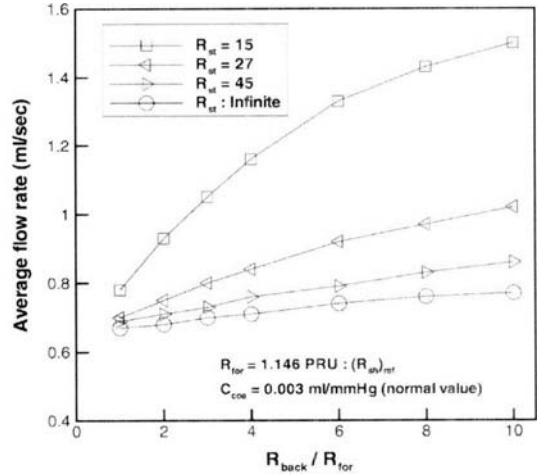

Fig. 11 LAD flow rate as a function of the ratio of backward resistance to forward resistance, R_{back}/R_{for}. Here, R_{sh} is in PRU

stenosis resistance decreases, going from one curve to the next. For any given stenosis severity, as the resistance ratio increases, the flow rate also increases. However, the rate of increase slows as the ratio increases further. We conducted parametric studies varying the ratio of backward resistance to forward resistance (the resistance ratio), as presented in Fig. 11. One interesting finding can be extracted from the combined results of Figs. 10 and 11. In Fig. 10, it is clear that if $R_{st} = 15$ PRU, the patient is better off without an LV-LAD conduit, since the flow rate is greatest for R_{sh} approaching infinity. By contrast, Fig. 11 shows that this same patient benefits considerably from the placement of a conduit if the resistance ratio is large. For example, if $R_{back}/R_{for} = 10$, the LAD flow rate is nearly 1.5 ml/s, which is much greater than the non-shunt flow of about 1 ml/s. It remains to be seen if a conduit with such large asymmetry can be produced.

To assess the effect of the compliance of the coronary artery in the case of asymmetric resistance, normal and high-capacitance cases were compared (Fig. 12). Higher capacitance leads to somewhat greater flow rates at the same resistance
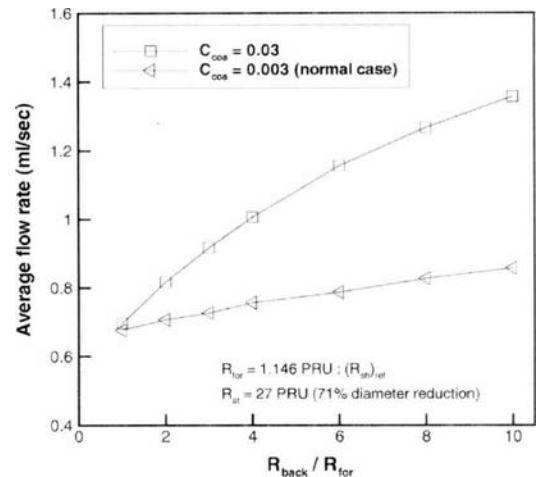

Fig. 12 LAD flow rate as a function of the resistance ratio R_{back}/R_{for}. Here, C_{coa} is in ml/mmHg

ratio and the gradient of the increase in flow rate is much steeper than that of the normal capacitance.

Since the fluid dynamics within the shunt is important for the hemodynamics aspects of the device, we have therefore presented more detailed, three-dimensional computations to assess the flow patterns in a shunt with a constant diameter. A commercial finite element package ADINA (Automatic Dynamics Incremental Nonlinear
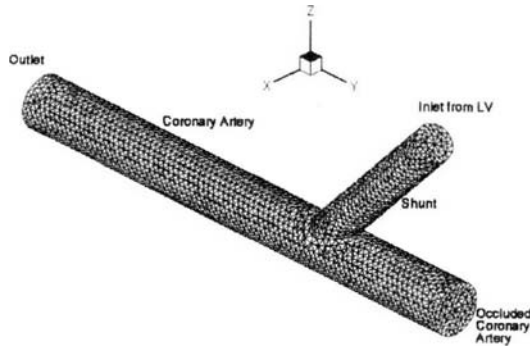
Fig. 13 Schematic of the computational model and the surface mesh at 45° shunt angle. The total number of nodes and elements used in this model are 13923 and 65173, respectively
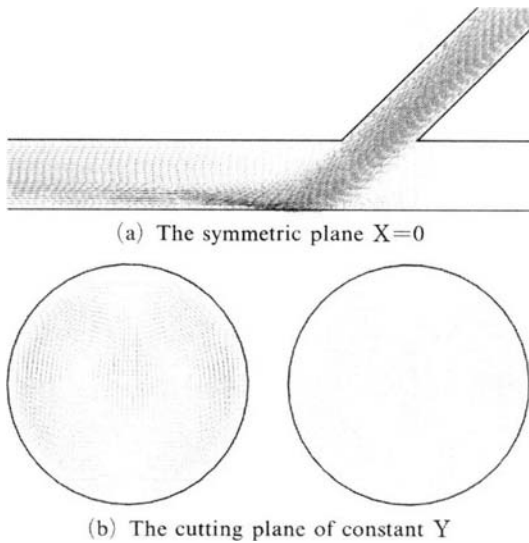

(a) The symmetric plane X=0

(b) The cutting plane of constant Y

Fig. 14 Velocity vectors

Analysis) (Bathe et al., 1995) is employed to simulate the fluid dynamics. For the boundary conditions we utilize the simulation result of coronary circulation with the artery totally blocked. The time varying pressures and flow rates at the left ventricle are applied to the shunt inlet boundary. Maximum Reynolds number in the shunt during a cardiac cycle is about 300 where Reynolds number is based on the shunt diameter and mean velocity in the inlet. The computational model in this study is depicted in Fig. 13 showing the bypass shunt connecting the occluded coro-

nary artery with the left ventricle. An unstructured tetrahedral mesh is used having four velocity and four pressure nodes. Fig. 14(a) depicts the velocity vectors at the symmetric cutting plane as a function of the shunt angle at the time of maximum inlet flow rate in. A large recirculating region can be seen near the junction. The velocity vectors in the cross-sectional planes at the proximal and at the distal part of the occluded coronary artery are shown in Fig. 14(b), showing significant secondary flow. This indicates the formation of two counter-rotating vortices in the artery. This secondary flow is attenuated as it moves into downstream.

4. Conclusions

In this study, we determined the computational results for the hemodynamics of a conduit connecting the left ventricle and left descending coronary artery. To delineate the effect of the conduit, we implemented a computational code that can simulate the system dynamics of the coronary circulation after inserting the conduit. Many critical cases were evaluated using this code, and we compared these results with available numerical and experimental data. Parametric studies of the simulation following insertion surgery were conducted. The computational results showed that the minimum shunt resistance produces the greatest flow with LAD occlusion. Moreover, distal vessels must be dilated maximally for effective myocardial perfusion. For a shunt with symmetric resistance, stenoses with a resistance less than 27 PRU (<71% diameter reduction) do not benefit from shunt placement. In all situations with a symmetric resistance in which a shunt is beneficial, the greatest benefit is derived with the smallest resistance. We conducted parametric studies varying the ratio of the backward resistance to the forward resistance. These studies indicated that the flow rate increases as the stenosis resistance decreased, going from one curve to the next. For any given stenosis severity, the flow rate increased with the resistance ratio. However, the rate of increase slows as the ratio increases further.

References

Bathe, K. J., Zhang, H., Wang, M. H., 1995, "Finite Element Analysis of Incompressible and Compressible Fluid Flows with Free Surfaces and Structural Interactions," *Computers and Structures*, 56, No. 2/3, pp. 193~213.

Beyar, R., Guerci, A. D., Halperin, H. R., Tsitlik, J. E., Weisfeldt, M. L., 1989, "Intermittent Coronary Sinus Occlusion After Coronary Arterial Ligation Results in Venous Retroperfusion," *Circ Res*, Vol. 65, No. 3, pp. 695~707.

Beyar, R., Caminker, R., Manor, D. and Sideman, S., 1993, "Coronary Flow Patterns in Normal and Ischemic Hearts : Transmyocardial and Artery to Vein Distribution," *Ann Biomed Eng*, Vol. 21, No. 4, pp. 435~458.

Boeksteqers, P., Raake, P., Al Ghobainy, R., Horstkotte, J., Hinkel, R., Sandner, T., Wichels, R., Meisner, F., Thein, E., March, K., Boehm, D. and Reichenspurner, H., 2002, "Stent-based Approach for Ventricle-to-coronary Artery Bypass," *Circulation*, Vol. 106, No. 8, pp. 1000-1006.

de Zeeuw, S., Borst, C., Grundeman, P. F., 2004, "Myocardial Blood Supply Through a Direct Left Ventricle-coronary Artery Shunt is not Aided by Augmented Coronary Capacitance," *J Thorac Cardiovasc Surg*, Vol. 127, No. 6, pp.1751~1758.

Feigl, E. O., 1989, Coronary Circulation. Textbook of Physiology. Vol. 2, 21st ed. Philadelphia, Pa : WB Saunders Co, pp. 933~950.

Frazier, O. H., March, R. J. and Horvath, K. A., 1999, "Transmyocardial Revascularization with a Carbon Dioxide Laser in Patients with End-stage Coronary Artery Disease," NEJM, 341, pp. 1021-1028.

Heldt, T., Shim, E. B., Kamm, R. D., Mark, R. G., 2002, "Computational Modeling of Cardiovascular Response to Orthostatic Stress," *J Appl Physiol*, Vol. 92, No. 3, pp. 1239~1254.

Rooz, E., Wiesner, T. F., Nerem, R. M., 1985, "Epicardial Coronary Blood Flow Including the Presence of Stenoses and Aorto-coronary Bypasses — I : Model and Numerical Method," *J Biomech Eng*, Vol. 107, No. 4, pp. 361~367.

Schreiner, W., Neumann, F. and Mohl, W., 1990, "Simulation of Coronary Circulation with Special Regard to the Venous bed and Coronary Sinus Occlusion," *J. Biomed. Eng.*, Vol. 12, pp. 429~443.

Shim, E. B., Youn, C. H., Heldt, T., Kamm, R. D. and Mark, R. G., 2002, "Computational Modeling of the Cardiovascular System After Fontan Procedure," *Lecture Notes in Computer Science*, 2526, pp. 105~114.

Suehiro, K., Shimizu, J., Yi, G-H., Zhu, S-M., Gu, A., Sciacca, R.R., Wang, J. and Burkhoff, D., 2001, "Direct Coronary Artery Perfusion from the Left Ventricle," *J Thorac Cardiovasc Surg*, 121, pp. 307~15.

Tweden, K. S., Eales, F., Cameron, J. D., Griffin, J. C., Solien, E. E. and Knudson, M. B., 2000, "Ventriculocoronary Artery Bypass (VCAB), a Novel Approach to Myocardial Revascularization," *Heart Forum*, 3. pp. 1~8.

Appendix A : Detailed formulation of the coronary circulation analysis

In this section, we present the detailed expressions used in the computational procedure to simulate coronary circulation. A schematic diagram of the computational code is represented in Fig. 3.

Variables

P   : Pressure (mmHg)
q   : Flow rate (ml/sec)
R   : Resistance (mmHg sec/ml=PRU)
C   : Compliance (ml/mmHg)
D   : Diode or check valve
V   : Compartmental volume (ml)

Subscripts

lv   : Left ventricle
ao   : Aortaa
st   : Stenosis of coronary arteries
by   : Bypass connection from the left ventricle
sh   : Conduit connection from the left ventricle
for : Conduit forward direction
back : Conduit backward direction
coa : Coronary arterioles
coc : Coronary capillaries

imp : Intra-myocardium
cov : Coronary veins
ra : Right atrium

The coronary circulation consists of three compartments : the coronary arteries, capillaries, and veins. The effects of myocardial muscle contraction or relaxation are produced by temporal variation in the bias pressure $P_{imp}(t)$. Therefore, the flow rates between the respective compartments are :

$$q_{st} = (P_a - P_{st})/R_{st} \qquad (A1)$$

$$q_{sh} = (P_{lv} - P_{st})/R_{sh} \begin{cases} R_{sh} = R_{for} & \text{if } P_{lv} > P_{st} \\ R_{sh} = R_{back} & \text{if } P_{lv} < P_{st} \end{cases} \quad (A2)$$

$$q_{coa} = \begin{cases} (P_{coc} - P_{coc})/R_{coa} & \text{if } P_{coa} > P_{coc} \\ \dfrac{(P_{coa} - P_{coc})}{(R_{coa} + \beta/V_{coc}^2)} & \text{otherwise} \end{cases} \quad (A3)$$

For the conduit resistance in Eq. A2, the resistance values of the conduit can be changed according to the direction of flow. The forward and backward resistances are shown in Fig. 2. In Eq. A3, the flow rate to capillaries may be either forward (i.e., $q_{coa} > 0$) or retrograde, depending on the sign of the pressure gradient. However, reverse flow ceases as the capillary volume approaches zero, since nothing then remains to be squeezed out. Moreover, as the capillary vessels are compressed, their resistance increases and they will throttle the flow. Accordingly, for a negative pressure gradient, Eq. A3 reduces backward flow to zero as the capillary volume approaches zero. The constant $\beta = 1$ (unit : mmHg· $s^{-1} \cdot ml^{-1}$) is adopted from the paper of Schreiner et al.(1990). For flow into the veins and right atrium, a similar approach can be applied, producing the following two equations.

$$q_{coc} = \begin{cases} \dfrac{(P_{coc} - P_{cov})}{(R_{coc} + 1/V_{coc}^2)} & \text{if } P_{coc} > P_{cov} \\ \dfrac{(P_{coc} - P_{cop})}{R_{coc} + \beta/V_{cov}^2} & \text{otherwise} \end{cases} \quad (A4)$$

$$q_{cov} = \begin{cases} \dfrac{(P_{cov} - P_{ra})}{(R_{cov} + \beta/V_{cov}^2)} & \text{if } P_{cov} > P_{ra} \\ \dfrac{(P_{cov} - P_{ra})}{R_{cov}} & \text{otherwise} \end{cases} \quad (A5)$$

The state form of the node equations can be written in terms of these flow rates.

(a) Conservation of mass at the coronary artery node

$$q_a + q_{sh} = q_{coa} + q'_{coa} \qquad (A6)$$

where

$$q'_{coa} = C_{coa} \frac{dP_{coa}}{dt} \qquad (A7)$$

$$\therefore \ \frac{dP_{coa}}{dt} = \frac{(q_{st} + q_{sh}) - q_{coa}}{C_{coa}} \qquad (A8)$$

(b) At the coronary capillaries node

$$q_{coa} = q_{coc} + q'_{coc} \qquad (A9)$$

where

$$q'_{coc} = C_{coc} \frac{d(P_{coc} - P_{imp})}{dt} \qquad (A10)$$

$$\frac{dP_{coc}}{dt} = \frac{q_{coa} - q_{coc}}{C_{coc}} + \frac{dP_{imp}}{dt} \qquad (A11)$$

(c) Capillary volume can be obtained using the relation

$$V_{coc} = C_{coc}(P_{coc} - P_{imp}) \qquad (A12)$$

(d) Mass conservation at the coronary veins node

$$q_{coc} = q_{cov} + q'_{cov} \qquad (A13)$$

where

$$q'_{cov} = C_{cov} \frac{dP_{cov}}{dt} \qquad (A14)$$

$$\therefore \ \frac{dP_{cov}}{dt} = \frac{q_{coc} - q_{cov}}{C_{cov}} \qquad (A15)$$

For the capillary veins, venous pressure is calculated from the pressure-volume relation :

$$P_{cov} = V_{coc} C_{cov}^0 e^{\sigma(V_{cov} - V_{cov}^0)} \qquad (A16)$$

corresponding to a volume-dependent compliance, defined as the derivative of V_{cov} with respect to P_{cov} :

$$C_{cov}(V_{cov}) = \frac{dV_{cov}}{dP_{cov}} = C^0(1 + \sigma V_{cov})^{-1} e^{-\sigma(V_{cov} - V_{cov}^0)} \qquad (A17)$$

Here, V_{cov}^0, C_{cov}^0 are the reference venous volume and compliance, respectively, and σ is the slope of the change in compliance.